Mon. Not. R. Astron. Soc. **359,** 1549–1556 (2005) doi:10.1111/j.1365-2966.2005.08993.x

Tentative detection of warm intervening gas towards PKS 0548-322 with *XMM–Newton*

X. Barcons,[1⋆] F. B. S. Paerels,[2] F. J. Carrera,[1] M. T. Ceballos[1] and M. Sako[3]

[1]*Instituto Física de Cantabria (CSIC-UC), 39005 Santander, Spain*
[2]*Columbia Astrophysics Laboratory, Columbia University, 538W, 120th Street, New York NY 10027, USA*
[3]*Stanford Linear Accelerator Centre, 2575 Sand Hill Road M/S 29, Menlo Park, CA 94025, USA*

Accepted 2005 March 7. Received 2005 February 28; in original form 2004 October 4

ABSTRACT

We present the results of a long (∼93 ks) *XMM–Newton* observation of the bright BL-Lac object PKS 0548-322 ($z = 0.069$). Our *Reflection Grating Spectrometer* (RGS) spectrum shows a single absorption feature at an observed wavelength $\lambda = 23.33 \pm 0.01$ Å, which we interpret as O VI Kα absorption at $z = 0.058$, i.e. ∼3000 km s^{-1} from the background object. The observed equivalent width of the absorption line, ∼30 mÅ, coupled with the lack of the corresponding absorption edge in the EPIC pn data, implies a column density of $N_{\rm O\,VI} \sim 2 \times 10^{16}$ cm^{-2} and turbulence with a Doppler velocity parameter $b > 100$ km s^{-1}. Within the limitations of our RGS spectrum, no O VII or O V Kα absorption are detected. Under the assumption of ionization equilibrium by both collisions and the extragalactic background, this is only marginally consistent if the gas temperature is $\sim 2.5 \times 10^5$ K, with significantly lower or higher values being excluded by our limits on O V or O VII. If confirmed, this would be the first X-ray detection of a large amount of intervening warm absorbing gas through O VI absorption. The existence of such a high column density absorber, much stronger than any previously detected one in O VI, would place stringent constraints on the large-scale distribution of baryonic gas in the Universe.

Key words: techniques: spectroscopic – galaxies: active – X-rays: galaxies.

1 INTRODUCTION

Current cosmological models restrict the baryon fraction in the Universe to a few per cent of its total matter and energy content. A large fraction of that number of atoms, ions and electrons is strongly suspected to reside in the intergalactic medium. Lyman α clouds (including damped Lyman α absorption systems) are seen to dominate the baryon content of the Universe at high redshift (Storrie-Lombardi & Wolfe 2000), but at lower redshifts their number density and the subsequent contribution to the ordinary matter content of the Universe decrease.

Detailed simulations of the cosmological evolution of the baryons invariably show that the Lyman α absorbing gas at temperatures $\sim 10^4$ K undergoes shock heating at lower redshifts and its temperature rises to 10^5–10^7 K (Cen & Ostriker 1999; Fang & Canizares 2000; Cen et al. 2001; Davé et al. 2001). The baryons in the warm and hot intergalactic medium (WHIM) reach 40–60 per cent of the total baryon budget in the local Universe, according to the above simulations. Indeed, most of these WHIM baryons live in small sparse concentrations, and only those in the deepest potential wells (groups and clusters of galaxies) can be seen through their X-ray emission. For the remaining WHIM baryons, resonance absorption lines from highly ionized elements (O VI, O VII, O VIII, Ne IX, etc.) offer the best chance of detecting them (Hellsten, Gnedin & Miralda-Escudé 1998; Fang & Canizares 2000).

Tenuous gas is best detected by absorption rather than by emission, if a bright (and featureless) enough source can be found, typically an AGN. The limiting equivalent width detectable for a resonance absorption line is ultimately determined by the spectral resolution of the spectrograph in use (assuming proper channel oversampling of each resolution element) but is most often limited by the signal-to-noise (S/N) ratio. Very roughly, for a typical S/N ∼ 10 spectrum, where each spectral resolution element is sampled by a few channels, the weakest absorption line detectable has an equivalent width of the order of the width of one channel. For the Reflection Grating Spectrometer (RGS; den Herder et al. 2001) that we use in this paper, the spectral resolution of the first-order spectra is around 60 mÅ, and therefore with a good-quality spectrum we might hope to detect lines as weak as 10–20 mÅ. With the slightly higher spectral resolution grating spectrographs on *Chandra*, lines as weak as 5–10 mÅ can be detected, given sufficient signal-to-noise ratio.

In recent years there have been a number of detections of resonance absorption lines arising in the WHIM, both in the soft X-ray

⋆E-mail: barcons@ifca.unican.es

band (with *Chandra* and *XMM–Newton*) and in the far-ultraviolet band (with *FUSE*). A local component of the WHIM was first discovered by Nicastro et al. (2002) using *Chandra* and *FUSE* data towards PKS 2155-204. Rasmussen, Kahn & Paerels (2003) reported on the discovery of local O VII absorption towards PKS 2155-204, 3C273 and Mkn 421 with *XMM–Newton*. Fang, Sembach & Canizares (2003) confirmed the detection of a $z = 0$ O VII Kα line towards 3C273 with *Chandra*.

The detection of more distant intervening WHIM seen in absorption is so far very limited. Fang et al. (2002) detect an O VIII Kα absorber towards PKS 2155-204 at a redshift coincident with an enhanced galaxy density in a well-studied region of the sky. McKernan et al. (2003) detect O VIII Kα absorption towards the radio galaxy 3C120, which can be interpreted either as intervening gas at $z = 0.0147$ or as gas ejected by 3C120 at a velocity of $\sim$5500 km s^{-1}. The current status of the detection of features from the non-local WHIM has been recently compiled by Nicastro et al. (2005). In that work, it is hinted that WHIM absorption lines can account for the missing baryons in the low-redshift Universe.

In this paper we present observations of the BL-Lac object PKS 0548-322 at $z = 0.069$ (Fosbury & Disney 1976). Prior to that Disney (1974) had detected the presence of a group of galaxies at $z = 0.04$ around this object, suggesting that PKS 0548-322 might be a cluster member. Much more recent work by Falomo, Pesce & Treves (1995) found that there is indeed a cluster (A S549) around this BL-Lac object, but at its average redshift of $z = 0.069$. X-ray emission from this cluster is very complicated to detect and measure given the brightness of PKS 0548-322.

We first use the RGS spectra to search for absorption lines. The single unresolved line found is identified as O VI Kα at a redshift intermediate between that of the BL Lac and observer. We then use the EPIC pn spectrum to help constraining the column density and Doppler velocity parameter of the absorber. We conclude by examining the turbulence of the absorbing gas and its possible temperature under the assumption of ionization equilibrium.

2 THE *XMM–NEWTON* RGS DATA

2.1 The X-ray data

PKS 0548–322 was observed by *XMM–Newton* (Jansen et al. 2001) during its 520th revolution, starting on 2002 October 11, as part of the AO-2 science operations (Obsid number is 0142270101). The observation lasted for 94 500 s. According to the analysis of the light curves of the various X-ray instruments, the radiation environment conditions were good and with low background except for the last $\sim$10 ks where strong flaring appeared. The pipeline products that were delivered to us had been processed with version 5.3.3 of the *XMM–Newton* Science Analysis Software (SAS). However, all data products were reprocessed using version 6.0.0 of SAS. In addition, the reprocessing incorporated a number of effective area corrections with respect to the earlier pipeline processed data.

The *RGS1* and *RGS2* data were filtered for high-background flare intervals, following the data analysis threads under the *XMM–Newton* SOC pages.[1] This resulted in 84 600 s of good exposure time for both spectrographs. Both spectrographs were operated in high event rate mode.

The spectra of order -1 and -2 for PKS 0548-322 were detected in both spectrographs. The second-order spectra, however, had very few counts and were ignored in this work. The resulting first-order spectra (in bins of width around 5 mÅ in the central part of the spectra) have a variable signal-to-noise ratio across the spectrum, which ranges from virtually zero below 6 Å and above 35 Å to a peak value of around $\sim$4–5 at wavelengths of $\sim$15–20 Å.

The search for absorption lines in the RGS spectra needs to start with the determination of the continuum level. In order to perform this, we have smoothed the spectra by grouping both the RGS1 and RGS2 data in bins containing at least 50 counts. The regions below 7 Å and above 35 Å, where the sensitivity of the RGS is very small, have been excluded from any further consideration. The determination of a good local continuum level is crucial to assessing the significance of any putative absorption line, and therefore we have restricted the continuum fits to patches of the RGS spectra where the residuals do not show any large trends.

To this end we have fitted separately the RGS spectra at both sides of the non-functioning CCDs. The RGS1 continuum has been determined independently in the 7–12 and 15–35 Å regions, and the RGS2 continuum has been determined independently at 7–20 and 24–35 Å. As is customary, we have used a single power-law spectrum absorbed by a Galactic column of 2.21×10^{20} cm^{-2}, but in reality any smooth function could have been used. [Note that in similar optical/ultraviolet (UV) studies, splines are often used to take into account the possible presence of weak broad emission line complexes.] The standard fitting routine XSPEC, version 11.2 (Arnaud 1996) was used throughout. The fitted parameters, along with the corresponding χ^2 values, are presented in Table 1. It is clear that although an absorbed power law does not provide a good enough fit to the full band, this model delivers a much more acceptable fit when restricted to either side of the non-functioning CCDs in both spectrometers. We will elaborate further on the continuum fitting in Section 2.3.

2.2 Searching for absorption lines

Detecting absorption lines in a noisy spectrum is a difficult task. We have taken the ratio of the data to the continuum model fitted with the binned data, but in the original non-grouped format, to search for absorption lines. We have chosen the code EQWID, kindly provided to us by Saskia Besier at the University of New South Wales (Australia). This code searches for significant 'connected' regions deviating from the continuum, knowing the spectral resolution. There are only two absorption features in the four spectral patches that have been explored, which are detected with significance above 3σ. One of them (with a centroid at 26.12 Å) is actually narrower (50 mÅ) than the spectral resolution of the RGS1 (60 mÅ), and is just significant at the 3σ level. All of this suggests that this is a non-real feature and in what follows we ignore it. There is, therefore, only one absorption-line candidate detected by the EQWID software, with a centroid at $\lambda = 23.33 \pm 0.014$ Å, with a FWHM of 74 ± 19 mÅ

Table 1. Fits to various wavelength regions with a power law absorbed by the Galactic column.

Instrument	λ range (Å)	Γ	χ^2/d.o.f.	$N_{\rm knots}$ [a]
RGS1+2	5–35	1.74 ± 0.02	2160.26/1351	–
RGS1	5–35	1.74 ± 0.02	1051.40/648	–
RGS1	5–15	2.00 ± 0.12	196.55/131	10
RGS1	15–35	1.34 ± 0.05	538.07/458	20
RGS2	5–35	1.74 ± 0.02	1059.15/699	–
RGS2	5–20	1.98 ± 0.04	599.63/499	14
RGS2	24–35	0.98 ± 0.18	239.10/195	14

[a] Number of knots used in the spline fit.

[1] http://xmm.vilspa.esa.es

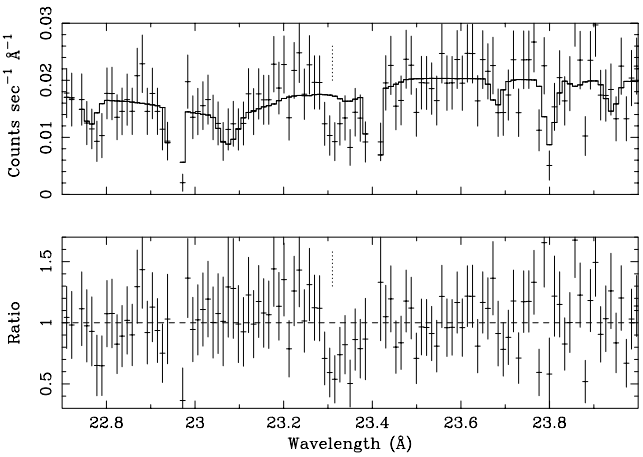

Figure 1. A portion of the RGS1 spectrum, fitted to a power law absorbed by the Galaxy, and the ratio of the data to the model. The feature at $\lambda = 23.33$ Å is the only significant feature in the whole of the RGS1 and RGS2 spectra that has a FWHM equal to or larger than the spectral resolution.

and a measured equivalent width of 32.3 ± 7.8 mÅ as returned by that code (1σ errors). The significance attributed to this detection is $\sim 3.7\sigma$. Unfortunately, the RGS2 data does not cover that region, due to the failure of the corresponding CCD (number 4) early in the mission.

Fig. 1 shows a relevant portion of the RGS1 spectrum, where the absorption line can be seen. There is a feature in the effective area at ∼23.35 Å which de Vries et al. (2003) attribute to an 1s–2p oxygen transition in the instrument. This feature occurs at a slightly, but significantly longer wavelength. The wavelength discrepancy between the instrumental absorption feature, and the feature we detect in our source amounts to ∼0.02 Å, or slightly more than one-third of an RGS resolution element. The wavelength scale has been calibrated to much higher accuracy (8 mÅ; den Herder et al. 2001). In addition, as we will show below, the measured equivalent width is significantly larger than that of the instrumental feature; and the presence of the instrumental feature is of course explicitly taken into account in the quantitative spectral analysis. We conclude that a misidentification of the feature in PKS0548-322 is excluded.

To further our confidence, we have also inspected other high signal-to-noise ratio RGS spectra of extragalactic objects. Rasmussen et al. (2003) present RGS spectra of 3C273, PKS 2155-304 and Mkn 421. In all three cases an O VII Kα absorption line at $z = 0$ (21.60 Å) is seen, with equivalent width ∼15–26 mÅ, i.e. weaker than our detection. In these spectra, however, there are no features detected at around 23.33 Å. Section 2.3 presents a further test, based on splitting of our observations into two parts, which enhances the reliability of the detected feature.

2.3 More on the continuum and the significance of the absorption line

All of the previous study is based on the assumption that a power law absorbed by the Galactic column fits the RGS spectra well on either side of the non-functioning CCDs and that the calibration (specifically the effective area) is accurate enough. Indeed, the spectrum of PKS 0548-422 could have slight, local deviations from the above model and the calibration could still be affected by small-scale systematic effects. As has been mentioned, the way these issues are solved in optical/UV absorption-line studies is by fitting a local continuum (regardless of its physical meaning), often using splines. Visually, the continuum adopted so far around the putative feature appears a bit low, and this adds interest to this further analysis.

Therefore, we have taken the data to continuum ratio resulting from the fits to either side of the non-functioning CCDs in both spectrometers and tried to fit a spline to each one individually. A region around the absorption line and the instrumental feature ranging from 23.29 to 23.38 Å has been masked out from this study. In order to prevent overfitting, that could eventually follow statistical noise spikes and even potential absorption or emission features, we explored decreasing the χ^2 as a function of the number of knots adopted. We then decided to adopt a number of knots below which χ^2 was not monotonically decreasing. This number, an obvious function of the wavelength width of the fitted region, is also shown in Table 1. In all cases the spline fitting implies a substantial decrease in the χ^2 fit to a constant. The data-to-model ratio for the four spectral zones were then divided by the spline fits and this was then used for further investigation as explained in what follows.

The routine EQWID was run on the newly renormalized ratios. Two features were found with a formal significance above 3σ. One at $\lambda = 14.70 \pm 0.02$ has a too narrow width (FWHM of only 21 mÅ) to be consistent with a real absorption line and it is therefore excluded. The other one, is the same line found without refitting the continuum, with the same formal significance of 3.7σ, the same central wavelength $\lambda = 23.33 \pm 0.012$, a similar width of 86 ± 19 mÅ and a slightly larger equivalent width of 39 ± 8 mÅ. This latter difference is indeed due to the fact that the continuum fitted by the splines is slightly larger. However, we decided to be conservative and keep the values presented in the previous subsection, bearing in mind that the highly uncertain continuum could change the equivalent width of the line, probably upwards.

There is one further experiment we can perform with the data-to-model ratio renormalized to the continua spline fits, given the fact that the distribution of these ratios appears to be approximately Gaussian. This is to assess the real significance of the line detected, by means of Monte Carlo simulations. In order to perform this, we generated renormalized data-to-model ratio spectra within the same four spectral bands, by assuming that values for each channel are Gaussian distributed with a mean of 1 and a dispersion given by the errorbar of the data-to-model renormalized ratio in the real data. Note that since the signal-to-noise ratio varies significantly across the spectra and therefore we cannot use an overall value for the dispersion of the Gaussian.

We run 10 000 independent simulations, and on each one of them we run the EQWID software. We filtered out those features detected which have either a positive equivalent width (corresponding to an emission feature) or a width smaller than the resolution of the spectrometer (60 mÅ). With these filters, a total of 605 lines were detected in the 10 000 simulations with a formal significance above 3.7σ. This in practice means that the probability of the detected feature at $\lambda = 23.33$ being a random noise feature is 6 per cent. Indeed, this implies a real significance close to 2σ. We have not, however, inspected every individual spectrum where a fictitious absorption line has been detected by EQWID, but a random inspection of a few of them shows that many do not conform to the shape of an unresolved line and Voigt profile fitting either does not converge or results in a very poor fit. This implies that the real probability that the detected feature is real is actually higher than 2σ.

2.4 Identifying and measuring the absorption line

To characterize this absorption feature, we have first modelled the absorption feature by using the *notch* model in XSPEC, added to the

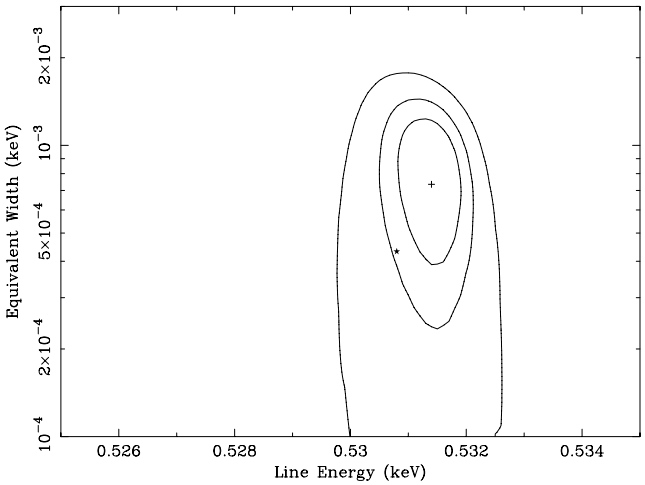

Figure 2. Best-fitting (+ sign) and confidence contours (1-, 2- and 3σ) for the line energy and equivalent width of a *notch* model fitted to the absorption line. The star sign represents the instrumental feature reported by de Vries et al. (2003), which is $\sim 2\sigma$ away, and in fact already accounted for in the continuum model.

absorbed power law. This *notch* model describes a fully saturated absorption 'square' feature, which is good enough in our case as the line appears unresolved. Inclusion of this new component in the fit to the RGS1 data in the 15–35 Å range produces a decrease in the $\chi^2_{\rm RGS}$ from 1800.17 (for 1620 degrees of freedom) to 1790.38 (for 1618 degrees of freedom). The F-test yields a significance of 98.8 per cent to this new component, slightly smaller than the significance of the line itself, as computed by EQWID. We attribute this to the inaccurate modelling of the line by this simple model. The best fit is found at a wavelength of $\lambda = 23.33^{+0.028}_{-0.023}$ Å and an equivalent width of 32^{+23}_{-16} mÅ (90 per cent errors for one single parameter). Fig. 2 shows the best fit and confidence contours for the observed equivalent width and absorption-line energy using the *notch* model, both in keV.

A further test has been performed in order to check whether an unfiltered bad event (or a set of them) in the region used to subtract the background could be responsible for the absorption feature. Note, however, that the shape of the absorption feature conforms to an approximately unresolved absorption line. To this end we split the RGS1 event file into two approximately equal halves in time, extracted the corresponding spectra, and computed χ^2 from the previously fitted models with and without the notch. The residuals of the model without the absorption modelled, both show a negative signal around $\sim$23.33 Å. Adding the notch model, for the first half of the observation χ^2 goes down from 1931.27 to 1926.83 when the absorption 'notch' is included with the parameters fitted to the overall spectrum, and for the second half χ^2 also decreases from 1895.56 to 1891.64. Therefore, although each half of the observation is not sensitive enough for a detection of the absorption feature, it is clear that a single bad event in the background region is not producing the observed line.

In order to identify the absorption line, assuming it is caused by intervening material, we made an extensive search for resonance lines associated with ground configurations, falling in the wavelength range from $\sim$23.33 Å (in the case where absorbing material occurs at $z = 0$) down to $\sim$21.82 Å (in the case where the line occurs at the redshift of PKS 0548 -322 $z = 0.069$). Note that the most often seen Kα transition of O VII (at a rest wavelength of 21.60 Å) falls outside this range by a large amount. In fact, for the line to be identified as O VII λ 21.60 the intervening material would have to be falling towards PKS 0548-322 at a velocity of $\sim$3000 km s^{-1}, which is far too large for a cluster of galaxies, especially for a poor cluster such as A S549. Note that a significant velocity difference (but in the opposite sense) has also been found by McKernan et al. (2003) in an O VIII Kα absorber towards 3C120. In that case (but not in ours, if the line is O VII Kα) there is a possible interpretation of the absorbing gas being in the jet and moving towards us.

The only physically meaningful option for that line is that it is O VI Kα λ 22.05, which has an oscillator strength of 0.576 (Pradhan et al. 2003). There is a further line in the doublet at λ 21.87, but its oscillator strength (0.061) is far too small to be detectable. Taking that interpretation, and the central wavelength measured by the notch model, the redshift of the absorbing gas is at $z = 0.058 \pm 0.001$.

Having established the nature of the line at 23.33 Å as O VI, it is natural to search for the most often seen O VII λ 21.60 line. In order to do this, we model the RGS1 data by including two notches tied down at the same (free) redshift, but assuming that one is O VI λ 22.05 and the other one O VII λ 21.60. The fit does not improve with the inclusion of the extra notch, but then we have explored a range in parameter space to establish limits on the equivalent width of the O VII absorption line. Fig. 3 shows the results, first in equivalent

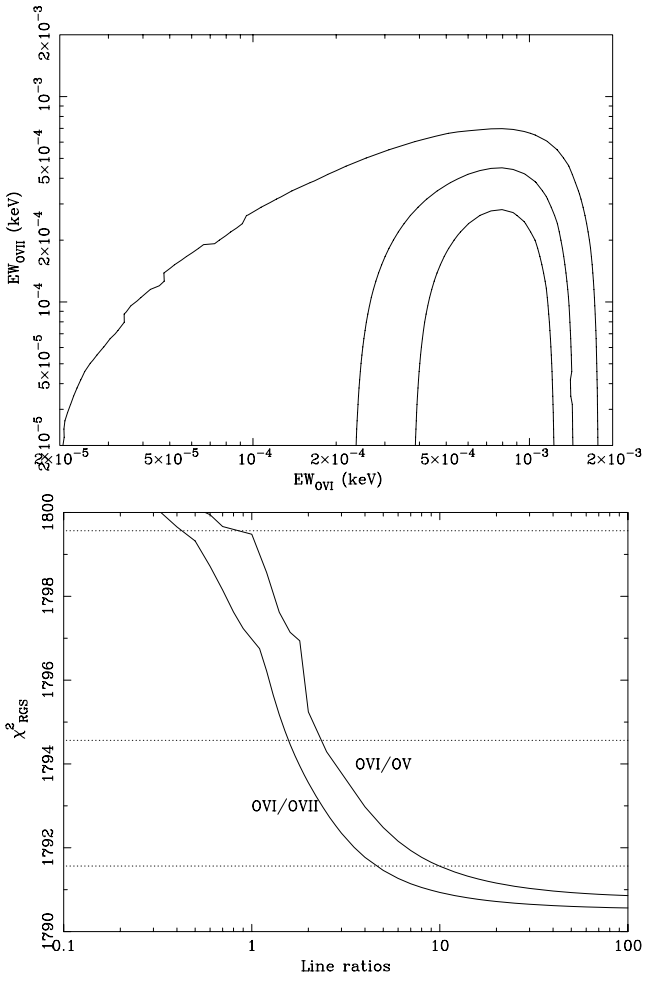

Figure 3. Top, confidence contours in the equivalent width of O VII and O VI parameter space, as obtained by simultaneously fitting two notches at the O VI and O VII Kα wavelengths and at the same redshift. Bottom, $\chi^2_{\rm RGS}$ (along with 1-, 2- and 3σ confidence levels) for O VI/O VII and O VI/O V equivalent width ratios, as derived from the same data.

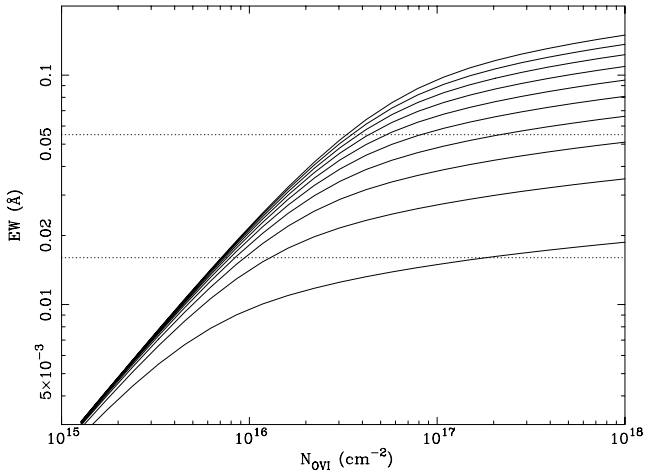

Figure 4. Growth curve for the O VI transition at 22.05 Å. The various curves (from bottom to top) correspond to Doppler parameters b from 50 to 500 km s^{-1} in 50 km s^{-1} steps. The horizontal lines denote the 90 per cent confidence region allowed by the data.

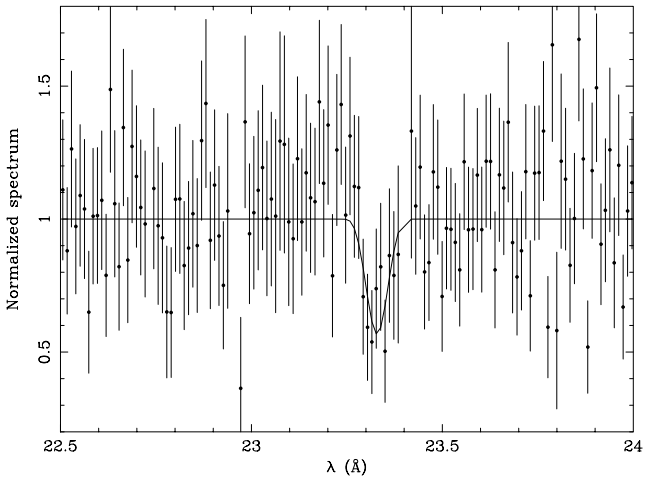

Figure 5. Fit to the ratio of the data to the continuum with a Voigt profile for the O VI line, Doppler broadened with $b = 200$ km s^{-1}.

width for O VI and O VII space and then for the O VI/O VII equivalent width ratio. The conclusion is that the O VI/O VII ratio is greater than 4.5, 1.5 and 0.4 at 1-, 2- and 3σ confidence, respectively. We have similarly constrained the equivalent width of the O V Kα line at 22.35 Å.

2.5 Profile fitting

Fig. 4 shows the growth curve for the O VI λ 22.05 transition, for a range of Doppler velocity broadening parameters b ($b = \sqrt{2}\sigma_v$, where σ_v is the velocity dispersion of the gas, assumed to be Maxwellian). Although the range of equivalent widths allowed at the 90 per cent level is large, it is clear that some level of Doppler broadening needs to be present or otherwise the implied value of $N_{\rm O\,VI}$ would be very large.

To gain further insight into the physical modelling of the absorption line, we have performed a Doppler-broadened Voigt profile fit to the data-to-model ratio in RGS1. The Voigt profile has been approximated using the formula by Whiting (1968) (accurate to better than 5 per cent), the thermal broadening is parametrized in terms of the b parameter and the spectrometer response has been modelled as a Gaussian of FWHM 750 km s^{-1} outside XSPEC (i.e. the model spectrum has been convolved with that Gaussian before being compared with the data-to-continuum ratio). Natural broadening (both radiative and auto-ionizing) is only relevant to very high column densities and it has been ignored here. Fits were restricted to the 22–24 Å range.

Since a fit with the three parameters ($N_{\rm O\,VI}$, b and z) left free yielded an undefined value for b ($b = 435 \pm 420$ km s^{-1}, 1σ error), we fixed b to a reasonable value of 200 km s^{-1} (see later). The best fit provides a substantial improvement of $\chi^2_{\rm Voigt}$, which goes from 182.4 for 171 data points to 164.94 with two fewer degrees of freedom. The F-test significance of this improvement is at the level of 99.98 per cent. The best-fitting values are $z = 0.0580^{+0.0008}_{-0.0006}$ and $\log N_{\rm O\,VI}({\rm cm}^{-2}) = 16.30 \pm 0.35$ (90 per cent errors). Fig. 5 shows the portion of the spectrum fitted, where it is seen that the fit is indeed satisfactory.

There is a previous, shorter *XMM–Newton* observation of PKS 0548-322 (Obsid number 0111830201), performed on 2001 October 3. The RGS spectra (which accumulate ∼48 ks of good exposure time each) have been presented and analysed by Blustin, Page & Branduardi-Raymont (2004), who do not find evidence for any significant absorption or emission features. Our own analysis of that data is entirely consistent with this. In fact, including an O VI absorption line with the parameters fixed to the above values, to the data-to-continuum ratio in the 22–24 Å region of the shorter exposure spectrum results in an *increase* of χ^2 from 59.13 (for 59 degrees of freedom) to 66.73. This increase is, however, too modest to exclude the possibility that the line is present in the noisier spectrum. There is also the possibility of a transient absorption feature, as discussed by Blustin et al. (2004) for broad absorption features in BL Lacs.

3 THE EPIC DATA

The two EPIC MOS detectors (Turner et al. 2001) operated in *fast uncompressed* mode, where the central chip (where the target was) is read as a single pixel. Since a proper background subtraction cannot be performed in this mode, we ignored the MOS data.

The EPIC pn detector (Strüder et al. 2001) was operated in large-window mode. After filtering out high-background episodes, the net exposure time where data were extracted went down to 77.2 ks. The spectrum of the source was extracted, following the SAS analysis threads, using a circle of radius ∼40 arcsec. The background spectrum was extracted from a ∼ five times larger region free from obvious sources, although in a different CCD chip and at a different detector y coordinate.

The count rate from the source region is 15.42 ct s^{-1} (without any pattern filtering), slightly above the count rate quoted in the *XMM–Newton* Users Handbook of 12 ct s^{-1} where pile-up starts to be relevant. In order to quantify the effects of pile-up, we used the SAS task EPATPLOT, which extracts the spectral distribution of the events with various patterns (singles, doubles, triples and quadruples) and compares that to a pile-up free model. The comparison shows that in the range 0.5–2 keV, pile-up has little affect, with an overall survival of single events of 99.2 per cent and an overall survival of double events of 98.7 per cent in that band. The differences between the predicted and observed spectral distributions do not exceed a few per cent at any particular channel in that band, which is of the order of the accuracy in the calibration of the EPIC pn. Hence we believe that the EPIC pn can be safely used in the 0.5–2 keV band. Above

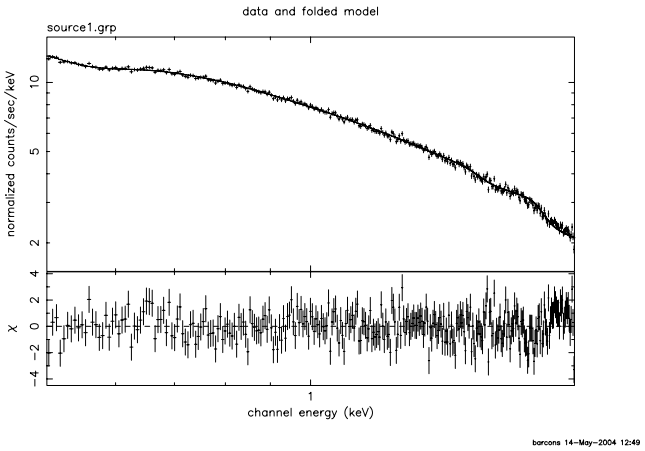

Figure 6. EPIC pn spectrum and deviations to a power-law model seen through Galactic absorption.

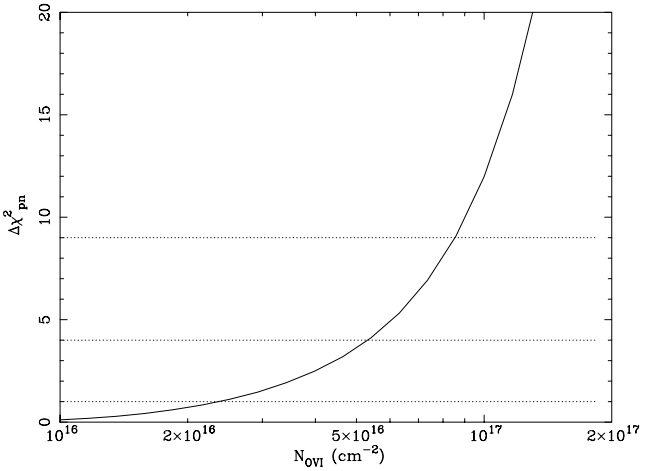

Figure 7. $\chi^2_{\rm pn}$ (the minimum has been subtracted) as a function of the column density $N_{\rm O\,VI}$ for the fit to the EPIC pn data in the 0.5–2 keV band to a power law absorbed by the Galaxy and an O VI absorber at $z = 0.058$, using the SIABS model (Kinkhabwala et al. 2005).

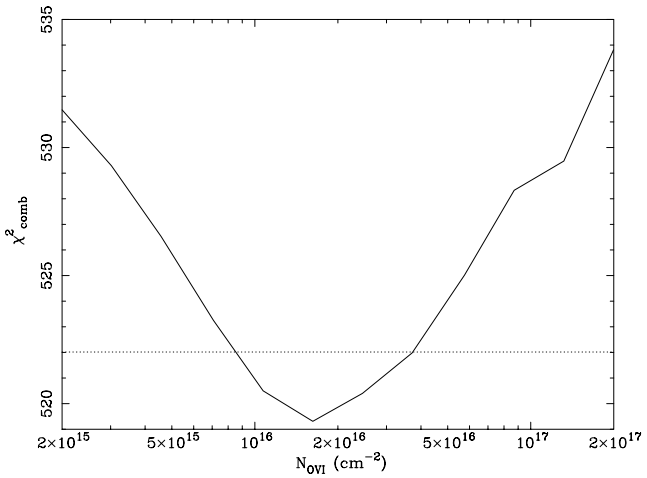

Figure 8. $\chi^2_{\rm comb}$ as a function of O VI column density, for a joint fit to the EPIC pn and the RGS1 ratio, where the Doppler velocity parameter b has been marginalized. The dotted line shows the 90 per cent confidence level.

that energy, and particularly around 2–3 keV, deviations from the non-piled-up model, exceed 10–15 per cent and consequently we ignore these data.

Hence we have used the 0.5–2 keV band photons, keeping only single and double events and only those with good spectral quality (FLAG = 0). A fit to a power law with Galactic absorption fixed at $N_H = 2.21 \times 10^{20}$ cm^{-2} yields a photon spectral index $\Gamma = 2.000 \pm 0.005$ (90 per cent errors). The unabsorbed flux in the 0.5–2 keV band is $S(0.5\text{–}2) = (1.865 \pm 0.004) \times 10^{-11}$ erg cm^{-2} s^{-1}.

Fig. 6 displays the spectral fit and the residuals, where there are no obvious deviations from the model (none exceeds 5 per cent at any energy in the 0.5–2 keV band). The fit is good, with $\chi^2_{\rm pn} = 354.51$ for 302 degrees of freedom, leaving a probability that the model is wrong of only 2 per cent. Our data does not show the previously claimed presence of spectral features in this object as seen by the *Einstein Observatory* (Madejski et al. 1991) and *ASCA* (Tashiro et al. 1994), which were tentatively interpreted as absorption edges. Such features, that were once thought to be universal among BL Lacs, are absent in the current data.

We have also tried to search explicitly for the presence of O VI in this spectrum, by using the SIABS absorption model (Kinkhabwala et al. 2005). This model keeps track of both the photoelectric absorption edge and the resonance absorption lines (modelled in terms of proper Voigt profiles) for a given ion species. Fixing the redshift of the absorber at the value measured in the RGS data ($z = 0.058$) and with a velocity dispersion corresponding to $b = 200$ km s^{-1} and with the RGS best fit $N_{\rm O\,VI} = 10^{16.3}$ cm^{-2}, $\chi^2_{\rm pn}$ improves by less than one unit. Fig. 7 shows $\chi^2_{\rm pn}$ as a function of $N_{\rm O\,VI}$ for the EPIC pn data, where it can be seen that the best-fitting values from the RGS data are within the 1σ level (assuming $b \sim 200$ km s^{-1}).

4 PROPERTIES OF THE ABSORBING GAS

4.1 Turbulence

Since large values of $N_{\rm O\,VI}$ are not allowed by the EPIC pn data, this poses additional constraints on the growth curve for O VI. In particular, a ∼30-mÅ absorption line resulting from a large column and very little turbulence (small b parameter) will be inconsistent with the EPIC pn spectrum.

To quantify this, we have explored a grid of values of $N_{\rm O\,VI}$ from 2×10^{15} to 2×10^{17} cm^{-2} and for the Doppler parameter b ranging from 50 to 1000 km s^{-1}. The RGS1 ratio to the continuum has been Voigt profile fitted in the range 22–24 Å and the EPIC pn spectrum has been fitted in the range 0.5–2 keV with a model consisting of a power law (absorbed by the Galactic H column) and a single O VI ion as defined by the model SIABS at $z = 0.058$. For each value of the parameters $N_{\rm O\,VI}$ and b the line centre in the RGS1 ratio is left as a free parameter and the power law in the EPIC pn data is also left free (two free parameters). We then minimize

$$\chi^2_{\rm comb} = \chi^2_{\rm Voigt} + \Delta\chi^2_{\rm pn}.$$

Formally, the minimum for $\chi^2_{\rm comb}$ is found at $\log N_{\rm O\,VI}({\rm cm}^{-2}) \sim 16.3$ and $b \sim 300$ km s^{-1}. Fig. 8 shows $\chi^2_{\rm comb}$ as a function of $N_{\rm O\,VI}$, considering b an uninteresting parameter, from which we derive $\log N_{\rm O\,VI} = 16.3 \pm 0.3$ (90 per cent errors). Fig. 9 shows $\chi^2_{\rm comb}$ as a function of b, where $N_{\rm O\,VI}$ has been marginalized. At 90 per cent confidence level $b = 300^{+500}_{-200}$ km s^{-1} (i.e. $b > 100$ km s^{-1}), but most importantly, very small values of b are very unlikely. In fact, $b < 50$ km s^{-1} is excluded at $>3\sigma$ confidence, implying that the

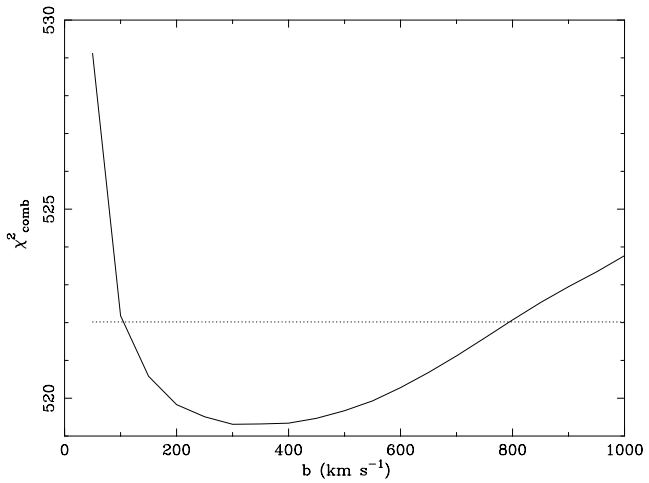

Figure 9. χ^2_{comb} as a function of the Doppler velocity parameter b, for a joint fit to the EPIC pn and the RGS1 ratio, where the O VI column density has been marginalized. The dotted line shows the 90 per cent confidence level.

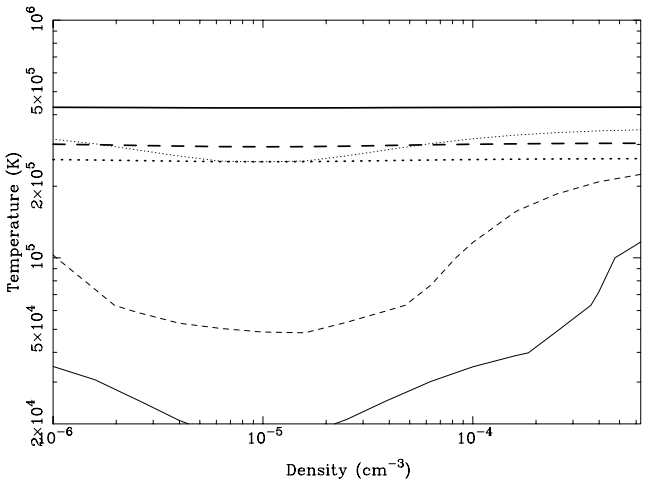

Figure 10. Region allowed in the temperature–density parameter space of the absorbing gas, as obtained from the constraints on the O VI/O VII (thin) and O VI/O V (thick) ratios: 1σ (solid), 2σ (dashed) and 3σ (dotted).

absorbing gas is turbulent. Very large values of b cannot be excluded by this analysis because combined with smaller values of the column density they can still fit the RGS absorption line.

4.2 Temperature

To test under what physical conditions the observed limits on the O VI/O VII and O VI/O V line ratios could take occur, we performed a number of CLOUDY runs (Ferland et al. 1998). We assume an optically thin cloud of gas confined by gravity, which is ionized both collisionally and by photoionization from the extragalactic background. We assumed the gas to be uniform, with 0.3 solar metallicity, temperature ranging from 10^4 to 10^7 K and particle density ranging from 10^{-6} to 10^{-3} cm^{-3}. The particle column density was fixed at a low but realistic value of 10^{20} cm^{-2}, but line ratios are independent of this under the optically thin conditions assumed. We adopt the simple extragalactic parametrization used by Nicastro et al. (2002), as a broken power law with energy spectral indices of 1.1 and 0.4, respectively, below and above 0.7 keV, normalized to 10 keV s^{-1} cm^{-2} sr^{-1} keV^{-1} at 1 keV (Barcons, Mateos & Ceballos 2000).

Fig. 10 shows the 1-, 2- and 3σ contours allowed in the density–temperature parameter space by the measured O VI/O VII and O VI/O V line ratios. Note that in displaying these contours, the line intensity ratios derived from the spectral fitting for the various Kα transitions, have been converted to column density ratios (which is what CLOUDY computes) by dividing each one by its oscillator strength (see Table 2). Collisional ionization dominates at densities $>10^{-5}$–10^{-4} cm^{-3}, but at the low-density end photoionization by the extragalactic background is the dominant ionization process. The 3σ upper limit on the gas temperature for O VI being seen but O VII being undetected is around 2.5×10^5 K, fairly independent of the density. This same value of the temperature is also approximately the 3σ *lower* limit for O VI being detected but O V being undetected.

The conclusion is that it is very difficult for gas under these conditions to show only O VI Kα absorption, without O V and/or O VII absorption.

Table 2. Wavelength and oscillator strength of the Kα transitions for the various oxygen ions considered here

Ion	λ (Å)	Oscillator strength
O V	22.35	0.565
O VI	22.05	0.576
O VII	21.60	0.694

5 DISCUSSION

The *XMM–Newton* RGS1 spectrum of PKS 0548-322 ($z = 0.069$) shows a single absorption feature, formally significant at the 3.7σ level. Monte Carlo simulations show that this significance is probably lower, but in any case higher than 2σ. Intervening O VI Kα absorption at $z = 0.058$ is the most likely interpretation of the absorption line. The equivalent width is ∼30–40 mÅ, a value that is of the order of that expected to be produced by a group or cluster. We do not find any significant absorption feature corresponding to the local WHIM ($z = 0$), nor to the putative cluster surrounding PKS 0548-322 ($z = 0.069$). Interpreting the detected absorption line in terms of O VII Kα absorption at the cluster redshift, would require the gas inflowing towards the BL Lac at a velocity close to 3000 km s^{-1}, which is at odds with the expectation that BL Lacs eject material towards the observer.

Despite previous claims on the presence of strong absorption edges (Madejski et al. 1991; Tashiro et al. 1994), we do not find such edges in the 0.5–2 keV EPIC pn spectrum of PKS 0548-322. Adopting the O VI identity for the absorption feature and combining the spectral fits to the RGS1 spectrum normalized to the continuum (Voigt profile fitting) with the EPIC pn data, we find that the absorber has an O VI column of $\log N_{\rm O\,VI}({\rm cm}^{-2}) = 16.3 \pm 0.3$, with significant turbulence (Doppler velocity parameter $b > 100$ km s^{-1} at 90 per cent confidence). The lack of O V and O VII Kα absorption lines in the RGS1 spectrum, however, imposes almost discrepant conditions on the temperature of the absorbing gas (assumed to be in ionization equilibrium by collisions and the extragalactic background). Marginal consistency is only achieved if the gas has a temperature of $T \sim 2.5 \times 10^5$ K.

If confirmed this would be the first detection of absorption by X-ray gas at such a low temperature. Simulations do show that

absorbing gas blobs in the WHIM should span a range of temperatures between 10^5 and 10^7 K (Davé et al. 2001), although so far only higher ionization species, probably corresponding to the highest temperatures in that range, have been detected. Chen et al. (2003) have specifically studied the cosmological distribution of O VI absorbers via simulations. Large column density systems, such as that tentatively detected here, are extremely rare according to the simulations. If confirmed, this would represent a strong challenge to our knowledge of the distribution of baryons on cosmic scales.

The fact that no other features associated either with the intervening absorber itself or the local WHIM are detected, points out for the need for a better S/N ratio high spectral resolution spectrum to confirm the existence of this peculiar absorber.

ACKNOWLEDGMENTS

This work is based on observations obtained with *XMM–Newton*, an ESA science mission with instruments and contributions directly funded by ESA member states and the USA (NASA). We are grateful to S. Besier and A. Fernández-Soto for help in the Voigt profile fitting. Comments from an anonymous referee, which resulted in a substantial improvement to the paper, are also appreciated. XB, FJC and MTC acknowledge partial financial support by the Spanish Ministerio de Educación y Ciencia, under project ESP2003-00812. FP acknowledges support from NASA, under grant NAG5-7737.

REFERENCES

Arnaud K. A., 1996, in Jacoby G. H., Barnes J., eds, ASP Conf. Ser. Vol. 101, Astronomical Data Analysis Software and Systems V. Astron. Soc. Pac., San Francisco, p. 17
Barcons X., Mateos S., Ceballos M. T., 2000, MNRAS, 316, L13
Blustin A. J., Page M. J., Branduardi-Raymont G., 2004, A&A, 417, 61
Cen R., Ostriker J. P., 1999, ApJ, 514, 1
Cen R., Tripp T. M., Ostriker J. P., Jenkins E. B., 2001, ApJ, 559, L5
Chen X., Weinberg D. H., Katz N., Davé R., 2003, ApJ, 594, 42
Davé R. et al., 2001, ApJ, 552, 473
den Herder J. W. et al., 2001, A&A, 365, L7
de Vries C. P., den Boggende A. J., den Herder J. W., Kaastra J. S., Paerels F. B., Rasmussen A. P., 2003, A&A, 404, 959
Disney M. J., 1974, ApJ, 193, L103
Falomo R., Pesce J. E., Treves A., 1995, ApJ, 438, L9
Fang T., Canizares C. R., 2000, ApJ, 539, 532
Fang T., Marshall H. L., Lee J. C., Davis D. S., Canizares C. R., 2002, ApJ, 572, L127
Fang T., Sembach K. R., Canizares C. R., 2003, ApJ, 586, L49
Ferland G. J., Korista K. T., Verner D. A., Ferguson J. W., Kingdon J. B., Verner E. M., 1998, PASP, 110, 761
Fosbury R. A. E., Disney M. J., 1976, ApJ, 207, L57
Hellsten U., Gnedin N. Y., Miralda-Escudé J., 1998, ApJ, 509, 56
Jansen F. A. et al., 2001, A&A, 365, L1
Kinkhabwala A., Behar E., Sako M., Gu M. F., Kahn S. M., Paerels F. B. S., 2005, ApJ, in press
McKernan B., Yaqoob T., Mushotzky R., George I. M., Turner T. J., 2003, ApJ, 598, L83
Madejski G. M., Mushotzky R. F., Weaver K. A., Arnaud K. A., Megan C. M., 1991, ApJ, 370, 198
Nicastro F. et al., 2002, ApJ, 573, 157
Nicastro F., Elvis M., Fiore F., Mathur S., 2005, Adv. Space Res., in press
Pradhan A. K., Chen G. X., Delhaye F., Nahar S., Oelgoetz J., 2003, MNRAS, 341, 1268
Rasmussen A., Kahn S. M., Paerels F., 2003, in Rosenberg J. L., Putman M. E., eds, The IGM/Galaxy Connection: the Distribution of Baryons at $z = 0$. ASSL Conf. Proc. Vol. 281. Kluwer, Dordrecht, p. 109
Storrie-Lombardi L. J., Wolfe A. M., 2000, ApJ, 543, 552
Strüder L. et al., 2001, A&A, 365, L18
Tashiro M., Ueda Y., Kii T., Makino F., Fujimoto R., Mushotzky R. F., Makishima K., Yamashita A., 1994, in Makino F., Ohashi T., eds, New Horizon of X-ray Astronomy – First Results From *ASCA*. Universal Academy, Tokyo, p. 343
Turner M. J. L. et al., 2001, A&A, 365, L27
Whiting E. E., 1968, J. Quant. Spectrosc. Radiat. Transfer, 8, 1379

This paper has been typeset from a TEX/LATEX file prepared by the author.